FABAD J. Pharm. Sci., 51, 2, 839-852, 2026
Doi: 10.55262/fabadeczacilik.1985225
RESEARCH ARTICLE

Design, Synthesis, and Preliminary Antiproliferative Evaluation of Benzimidazole-1,3,4-oxadiazole Hybrids Showing Preferential Activity in Breast Cancer Cell Lines

Mahmut GOZELLE[*°], Şevval YAMAN[**], Züleyha ARSLAN[***], Yaprak Dilber ŞİMAY DEMİR[****]

Design, Synthesis, and Preliminary Antiproliferative Evaluation of Benzimidazole-1,3,4-oxadiazole Hybrids Showing Preferential Activity in Breast Cancer Cell Lines

SUMMARY

In this study, a new series of benzylthio-substituted benzimidazole-1,3,4-oxadiazole hybrids was designed, synthesized, and evaluated for their biological activity. The title compounds, 2-((2-(benzylthio)-1H-benzimidazol-1-yl)methyl)-5-aryl-1,3,4-oxadiazoles (1-4), were prepared through a multistep synthetic route starting from 2-mercaptobenzimidazole. The synthesis involved S-benzylation, N-alkylation with ethyl chloroacetate, hydrazide formation, and $POCl_3$-mediated cyclodehydration with selected benzoic acid derivatives. The structures of the synthesized compounds were confirmed by FT-IR, ^{1}H NMR, ^{13}C NMR, and HRMS analyses. The antiproliferative activities of compounds 1-4 were investigated against A549 lung adenocarcinoma, MCF-7 estrogen receptor-positive breast cancer, and MDA-MB-468 triple-negative breast cancer cell lines using the MTT assay. Doxorubicin was used as the reference anticancer drug. The synthesized compounds did not show a meaningful cytotoxic effect against A549 cells, with cell viability remaining approximately 95-100% at 100 µM. In contrast, a more pronounced response was observed in breast cancer cells. At 100 µM, compounds 1-4 reduced cell viability to 44.25%, 57.25%, 37.75%, and 61.25%, in MCF-7 cells and to 46.25%, 61.00%, 39.00%, and 45.00% in MDA-MB-468 cells, respectively. Among the tested derivatives, compound 3, bearing a para-methoxy substituent, showed the most favorable activity profile in both breast cancer cell lines. In the DPPH assay, the compounds did not exhibit notable radical scavenging activity, suggesting that their antiproliferative effects are unlikely to be directly related to classical antioxidant behavior. Overall, these findings indicate that the benzimidazole-1,3,4-oxadiazole hybrid scaffold may provide a useful starting point for the development of breast cancer-oriented antiproliferative candidates.

Keywords: *Benzimidazole, oxadiazole, antiproliferative activity, breast cancer, MTT assay, DPPH.*

Benzimidazol-1,3,4-okzadiazol Hibritlerinin Tasarımı, Sentezi ve Meme Kanseri Hücre Hatlarında Tercihli Aktivite Gösteren Ön Antiproliferatif Değerlendirmesi

ÖZ

Bu çalışmada, benziltiyo sübstitüenti taşıyan yeni benzimidazol-1,3,4-okzadiazol hibrit bileşiklerinin tasarımı, sentezi ve biyolojik aktiviteleri değerlendirilmiştir. Hedef bileşikler olan 2-((2-(benziltiyo)-1H-benzimidazol-1-il)metil)-5-aril-1,3,4-okzadiazol türevleri (1-4), 2-merkaptobenzimidazolden başlanarak çok basamaklı bir sentez yolu ile hazırlanmıştır. Sentez süreci; S-benzilasyon, etil kloroasetat ile N-alkilasyon, hidrazit oluşumu ve seçilmiş benzoik asit türevleri ile $POCl_3$ aracılı siklodehidrasyon basamaklarını içermektedir. Sentezlenen bileşiklerin yapıları FT-IR, ^{1}H NMR, ^{13}C NMR ve HRMS analizleriyle doğrulanmıştır. Bileşik 1-4'ün antiproliferatif aktiviteleri A549 akciğer adenokarsinom, MCF-7 östrojen reseptörü pozitif meme kanseri ve MDA-MB-468 üçlü negatif meme kanseri hücre hatlarında MTT yöntemi ile araştırılmıştır. Doksorubisin referans antikanser ilaç olarak kullanılmıştır. Sentezlenen bileşikler A549 hücrelerinde belirgin bir sitotoksik etki göstermemiş ve 100 µM konsantrasyonda hücre canlılığı yaklaşık %95-100 aralığında kalmıştır. Buna karşılık, meme kanseri hücrelerinde daha belirgin bir yanıt gözlenmiştir. 100 µM konsantrasyonda bileşik 1-4, MCF-7 hücrelerinde hücre canlılığını sırasıyla %44,25, %57,25, %37,75 ve %61,25'e; MDA-MB-468 hücrelerinde ise sırasıyla %46,25, %61,00, %39,00 ve %45,00'e düşürmüştür. Seri içerisinde para-metoksi sübstitüenti taşıyan bileşik 3, her iki meme kanseri hücre hattında en olumlu aktivite profilini göstermiştir. DPPH testinde ise bileşikler belirgin bir radikal süpürücü aktivite göstermemiştir. Bu sonuç, gözlenen antiproliferatif etkinin klasik antioksidan davranışla doğrudan ilişkili olmayabileceğini düşündürmektedir. Genel olarak elde edilen bulgular, benzimidazol-1,3,4-okzadiazol hibrit iskeletinin meme kanseri odaklı antiproliferatif ajanların geliştirilmesi için değerli bir başlangıç noktası olabileceğini göstermektedir.

Anahtar Kelimeler: *Benzimidazol, okzadiazol, antiproliferatif aktivite, meme kanseri, MTT testi, DPPH.*

Received: 02.07.2026
Revised: 22.07.2026
Accepted: 25.07.2026

[*] ORCID: 0000-0003-0234-6577, Department of Pharmaceutical Chemistry, Faculty of Pharmacy, Gazi University, 06330 Ankara, Türkiye
[**] ORCID: 0009-0004-6026-8233, Department of Pharmaceutical Chemistry, Faculty of Pharmacy, Gazi University, 06330 Ankara, Türkiye
[***] ORCID: 0009-0004-1305-8137, Department of Pharmacology, Faculty of Pharmacy, Gazi University, 06330 Ankara, Türkiye
[****] ORCID: 0000-0002-8248-0268, Department of Pharmacology, Faculty of Pharmacy, Gazi University, 06330 Ankara, Türkiye

[°] Corresponding Author; Mahmut GOZELLE
E-mail: mgozelle@gazi.edu.tr

INTRODUCTION

Cancer is a highly heterogeneous disease group characterized by uncontrolled cell proliferation, resistance to cell death, invasion, and metastatic dissemination. Despite substantial advances in diagnosis and treatment, cancer remains one of the major causes of morbidity and mortality worldwide. According to GLOBOCAN 2022 estimates, nearly 20 million new cancer cases and approximately 9.7 million cancer-related deaths occurred globally. Lung cancer and female breast cancer were the most frequently diagnosed malignancies, accounting for approximately 12.4% and 11.6% of all new cancer cases, respectively (Bray et al., 2024). Breast cancer is particularly important in anticancer drug discovery because of its high incidence, biological heterogeneity, and variable response to therapy. In 2022, approximately 2.3 million new female breast cancer cases and around 670,000 breast cancer-related deaths were reported worldwide (Bray et al., 2024; Kim et al., 2025; Zhang et al., 2025).

Breast cancer is not a single disease entity, but a molecularly diverse malignancy classified mainly according to the expression of estrogen receptor (ER), progesterone receptor (PR), and human epidermal growth factor receptor 2 (HER2). This classification directly influences treatment selection and clinical outcome. While ER-positive tumors may respond to endocrine therapy and HER2-positive tumors can benefit from HER2-targeted agents, triple-negative breast cancer (TNBC) lacks ER, PR, and HER2 expression and therefore has limited targeted treatment options (Perou et al., 2000; Yin, Duan, Bian, & Yu, 2020). TNBC is generally associated with aggressive progression, early recurrence, and poor prognosis, highlighting the need for new compounds active against different breast cancer phenotypes (Yin et al., 2020; Zagami & Carey, 2022).

In the present study, A549, MCF-7, and MDA-MB-468 cell lines were selected to evaluate whether the synthesized compounds exhibit broad cytotoxicity or a cell-type-dependent activity profile. A549 cells were used as a representative non-small cell lung cancer/lung adenocarcinoma model with type II alveolar epithelial-like characteristics, KRAS G12S mutation, and wild-type EGFR status (Foster, Oster, Mayer, Avery, & Audus, 1998; Tsukumo, Naito, & Suzuki, 2020; Werner Alyssa, Kumar Avani, Charest Pascale, & Welch, 2023). In contrast, MCF-7 and MDA-MB-468 cells were included as biologically distinct breast cancer models. MCF-7 represents an ER-positive/luminal phenotype, whereas MDA-MB-468 is a basal-like/triple-negative breast cancer model lacking ER, PR, and HER2 expression and characterized by EGFR overexpression/amplification and PTEN loss (Dai, Cheng, Bai, & Li, 2017; Subik et al., 2010). Therefore, the combined use of A549, MCF-7, and MDA-MB-468 cells provides a rational experimental platform to determine whether the tested compounds act as broadly cytotoxic agents or display a more selective activity pattern toward breast cancer phenotypes, including both hormone receptor-positive and triple-negative models.

The design strategy of this study was based on the molecular hybridization of two pharmacologically valuable heterocyclic scaffolds: benzimidazole and 1,3,4-oxadiazole. Benzimidazole was selected as the main core because it is a privileged nitrogen-containing heterocycle with structural similarity to purine bases and the ability to interact with biological targets through hydrogen bonding, π–π stacking, hydrophobic interactions, and donor–acceptor contacts (Hagar, Abbas, Atef, Abdelhamid, & Abdel-Aziz, 2025). Its easy functionalization at the N-1, C-2, and 5/6 positions also allows modulation of lipophilicity, electronic properties, solubility, and target-binding capacity. The anticancer relevance of this scaffold is supported by benzimidazole-containing agents such as bendamustine, as well as by numerous experimental benzimidazole derivatives reported to act through DNA damage, kinase inhibition, tubulin modulation, apoptosis induction, and PARP-related mechanisms (Badawy, Bräse, Ali, Abdel-Aziz, & Abdel-Rahman, 2025; Hagar et al., 2025; Lalic et al., 2022; Lee, Tan, & Oon, 2023).

The 1,3,4-oxadiazole ring was incorporated as the second pharmacophoric unit because of its important bioisosteric and drug-like properties. This five-membered aromatic heterocycle can act as a bioisostere of ester, amide, and carbamate groups, potentially improving metabolic stability, polarity, and molecular geometry (Glomb, Szymankiewicz, & Świątek, 2018; Kumar, Patel, Chavers, Chang, & Shah, 2011; Stecoza et al., 2021). Moreover, its relatively rigid and planar structure may help orient pharmacophoric groups in a favorable conformation for target binding. The presence of a 1,3,4-oxadiazole motif in clinically relevant drugs, such as the HIV integrase inhibitor raltegravir, further supports the medicinal value of this scaffold (Gupta et al., 2026; Nachman et al., 2014). In anticancer research, 1,3,4-oxadiazole derivatives have been associated with several mechanisms, including inhibition of EGFR, VEGFR, thymidylate synthase, histone deacetylases, tubulin polymerization, and DNA-related pathways (De Oliveira, Lira, Barbosa-Filho, Lorenzo, & De Athayde-Filho, 2012; Glomb et al., 2018; Shajari & Eskandari, 2026).

Based on these considerations, the benzimidazole-1,3,4-oxadiazole hybrid framework (Singh et al., 2022) was designed to combine the target-binding potential of benzimidazole with the bioisosteric, electronic, and conformational advantages of the oxadiazole ring. This design was expected to generate structurally compact molecules capable of forming multiple interactions with cancer-related targets, while also allowing substituent-based optimization of lipophilicity and electronic distribution. In this hybrid system, the benzimidazole moiety may contribute to aromatic and hydrogen-bonding interactions, whereas the oxadiazole unit may function as a metabolically stable linker and pharmacophoric element. Thus, the design rationale was not merely to merge two heterocycles, but to create a multifunctional scaffold with potential activity against breast cancer cells.

Previous studies have shown that benzimidazole–1,3,4-oxadiazole hybrids represent a promising scaffold in anticancer drug discovery (Abd El-Meguid, Awad, & Anwar, 2019; Badawy et al., 2025; Çevik et al., 2025; Gunjan et al., 2024; Hagar et al., 2023; Quy et al., 2022). These compounds have been reported to exhibit cytotoxic activity against several cancer cell lines, including MCF-7, HeLa, A549, MDA-MB-231, HepG2, and PANC-1, with some derivatives reaching low micromolar IC_{50} values and inducing apoptosis-related effects. Structure–activity relationship studies indicate that antiproliferative activity is strongly affected by the substitution pattern on the benzimidazole ring, the aryl group attached to the oxadiazole moiety, linker characteristics, halogen substitution, and molecular lipophilicity. In particular, N-1 substituted benzimidazole derivatives and halogenated aromatic groups have often been associated with improved activity. Although benzimidazole-oxadiazole hybrids have generally shown broad cytotoxic effects, including activity against A549 lung cancer cells, the compounds in the present study displayed a different response profile. Their limited activity in A549 cells, together with more pronounced effects in MCF-7 and MDA-MB-468 breast cancer cells, suggests a cell type-dependent antiproliferative pattern and highlights the potential relevance of this scaffold for breast cancer-oriented compound development.

Accordingly, the present study aimed to synthesize and evaluate benzimidazole-1,3,4-oxadiazole hybrid compounds (Figure 1.) against A549 lung cancer cells and two molecularly distinct breast cancer cell lines, MCF-7 and MDA-MB-468. The inclusion of A549 cells enabled comparison with a non-breast cancer model, while MCF-7 and MDA-MB-468 allowed assessment of activity in ER-positive and triple-negative breast cancer phenotypes. Interestingly, the observation that the compounds were largely inactive in A549 cells but active in both breast cancer models suggests a breast cancer-oriented and cell-type-dependent cytotoxic profile rather than a nonspecific cytotoxic effect. This selective activity pattern provides a meaningful basis for further mechanistic studies focusing on apoptosis, oxidative stress, cell-cycle regulation, and dysregulated survival pathways in breast cancer.

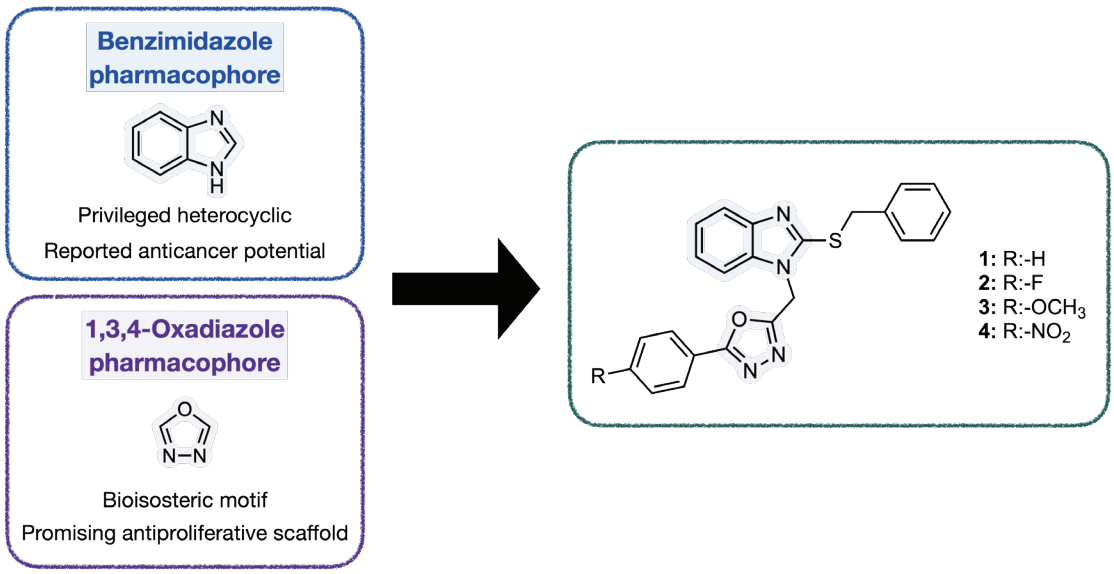

Figure 1. Design approach for benzimidazole-1,3,4-oxadiazole hybrid compounds

MATERIALS AND METHODS

Chemistry

All chemicals and solvents were purchased from commercial suppliers and used as received without further purification. The progress of the reactions was monitored by thin-layer chromatography (TLC) using silica gel 60 F_{254} aluminum-backed plates (Merck), and the spots were visualized under ultraviolet light at 254 and 365 nm. Mass spectrometric analyses were carried out on a Waters ACQUITY QDa II single-quadrupole mass detector equipped with an electrospray ionization (ESI) source operating in positive ion mode and coupled to a Waters ACQUITY UPLC H-Class system fitted with a photodiode array (PDA) detector (Waters Corporation, Milford, MA, USA). High-resolution mass (HRMS) measurements were obtained using a Waters LCT Premier XE time-of-flight mass spectrometer with an electrospray ionization source operating in positive mode (ESI^+), interfaced with an ACQUITY UPLC system (Waters Corporation, Milford, MA, USA). Chromatographic detection for HRMS analyses was performed at 254 nm. The purity of all title compounds was assessed by UPLC analysis and was found to exceed 97%. Infrared spectra (IR) were recorded on a PerkinElmer Spectrum 400 FT-IR/FT-NIR spectrometer equipped with a Universal ATR accessory, and the absorption bands are reported as wavenumbers (cm^{-1}). Nuclear magnetic resonance spectra (^1H and ^{13}C NMR) were acquired on a Bruker Avance Neo 500 MHz FT-NMR spectrometer. Tetramethylsilane (TMS) was used as the internal standard, and chemical shifts are expressed in parts per million (δ, ppm), while coupling constants (*J*) are reported in hertz (Hz). Melting points were determined using a Stuart SMP50 automatic melting point apparatus and are reported as observed values without correction.

Synthesis of intermediates

2-(Benzylthio)-1*H*-benzimidazole (**A1**)

2-Mercaptobenzimidazole (751 mg, 5 mmol) and benzyl chloride (632 mg, 5 mmol) were dissolved in acetone (35 mL) in the presence of potassium carbonate (1035 mg, 7.5 mmol). The reaction mixture was refluxed for 5 h, and the progress of the reaction was monitored by TLC. Upon completion, the reaction mixture was allowed to cool to room temperature and then poured into ice-cold water. The resulting precipitate was collected by vacuum filtration, washed with distilled water, and dried. The crude product was obtained in sufficient purity and used directly in the subsequent synthetic step without further purification.

Yield: 980 mg (82%); white solid. CAS No. 51290-77-8. Mp: 180.2-180.6 °C. MS (ESI^+) *m*/*z*: 241.0869 $[M+H]^+$.

Ethyl 2-(2-(benzylthio)-1*H*-benzimidazol-1-yl) acetate (**A2**)

Intermediate **A1** (980 mg, 4 mmol), ethyl chloroacetate (735 mg, 6 mmol), and potassium carbonate (1104 mg, 8 mmol) were dissolved in DMF (20 mL), and the reaction mixture was stirred at 100 °C. The progress of the reaction was monitored by TLC, and completion was observed after approximately 1 h. The reaction mixture was then cooled to room temperature and poured into ice-cold water. The resulting mixture was extracted with ethyl acetate, and the organic layer was washed with brine. After drying over anhydrous Na_2SO_4, the organic phase was removed under reduced pressure. The crude product was purified by column chromatography using n-hexane/ethyl acetate (80:20, v/v) as the eluent. Yield: 1111 mg (85%); colorless oil. CAS No. 1279115-87-5. MS (ESI^+) *m*/*z*: 327.0365 $[M+H]^+$.

2-(2-(Benzylthio)-1*H*-benzimidazol-1-yl)acetohydrazide (**A3**)

Intermediate **A2** (1000 mg, 3 mmol) and hydrazine hydrate (1152 mg, 18 mmol) were dissolved in ethanol (20 mL), and the reaction mixture was refluxed. The progress of the reaction was monitored by TLC, and completion was achieved after approximately 7 h. After completion, the reaction mixture was cooled to room temperature. The resulting precipitate was collected by vacuum filtration, washed with petroleum ether to remove impurities, and dried. The crude product was obtained in sufficient purity and used directly in the next synthetic step without further purification. Yield: 829 mg (88%); white solid. CAS No. 376605-23-1. Mp: 196.5-196.8 °C. MS (ESI^+) *m*/*z*: 313.0916 $[M+H]^+$.

General synthesis for title compounds (1-4)

Intermediate **A3** (1.0 equiv.) and the appropriate benzoic acid derivative (1.5 equiv.) were suspended in phosphorus oxychloride and heated at 80 °C. The progress of the reaction was monitored by TLC. Upon completion, the reaction mixture was cooled to room temperature and carefully poured into 10% aqueous sodium hydroxide solution. The resulting mixture was extracted with dichloromethane, and the organic phase was washed with brine, dried over anhydrous Na_2SO_4, filtered, and concentrated under reduced pressure. The crude residue was purified by column chromatography using dichloromethane/ethyl acetate (90:10, v/v), followed by a second purification using petroleum ether/acetone (85:15, v/v), affording the desired compounds **1**-**4**.

2-((2-(Benzylthio)-1*H*-benzimidazol-1-yl)methyl)-5-phenyl-1,3,4-oxadiazole (**Compound 1**)

Prepared according to the general procedure from intermediate **A3** (312 mg, 1.0 mmol) and benzoic acid (183 mg, 1.5 mmol). Yield: 64 mg (16%); white solid. Mp 142.0-142.5 °C. HRMS (ESI) *m*/*z*: calcd for $C_{23}H_{19}N_4OS$ $[M+H]^+$ 399.1280; found 399.1286. IR (ATR, cm^{-1}): 3087, 3060, 2923, 1608, 1575, 1493, 1443, 1280, 1255, 1237, 1087, 1070, 771, 747, 694. ^1H NMR (500 MHz, $CDCl_3$) δ 7.93 (d, *J* = 7.2 Hz, 2H), 7.78 (dd, *J* = 6.3, 3.0 Hz, 1H), 7.54 (t, *J* = 7.4 Hz, 1H), 7.47 (t, *J* = 7.4 Hz, 3H), 7.43 (d, *J* = 6.3 Hz, 2H), 7.36-7.24 (m, 5H), 5.51 (s, 2H), 4.69 (s, 2H). ^{13}C NMR (126 MHz, $CDCl_3$) δ 165.89, 160.63, 151.05, 143.12, 136.49, 135.44, 132.18, 129.08, 128.77, 127.89, 127.07, 123.21, 123.11, 123.04, 118.81, 109.17, 38.54, 38.13.

2-((2-(Benzylthio)-1*H*-benzimidazol-1-yl)methyl)-5-(4-fluorophenyl)-1,3,4-oxadiazole (**Compound 2**)

Prepared according to the general procedure from intermediate **A3** (312 mg, 1.0 mmol) and 4-fluorobenzoic acid (210 mg, 1.5 mmol). Yield: 50 mg (12%); white solid. Mp 130.7-131.0 °C. HRMS (ESI) *m*/*z*: calcd for $C_{23}H_{18}FN_4OS$ $[M+H]^+$ 417.1185; found 417.1192. IR (ATR, cm^{-1}): 3105, 3085, 3062, 2976, 1608, 1575, 1493, 1444, 1342, 1298, 1237, 1185, 1082, 1010, 842, 813, 772, 759, 732, 695. ^1H NMR (500 MHz, $CDCl_3$) δ 7.90 (dd, *J* = 9.0, 5.2 Hz, 2H), 7.75 (d, *J* = 7.2 Hz, 1H), 7.49-7.36 (m, 3H), 7.34-7.23 (m, 5H), 7.14 (t, *J* = 8.7 Hz, 2H), 5.48 (s, 2H), 4.66 (s, 2H). ^{13}C NMR (126 MHz, $CDCl_3$)

δ 165.07, 165.03 (d, *J* = 253.9 Hz), 160.65, 151.03, 143.14, 136.52, 135.43, 129.42 (d, *J* = 8.7 Hz), 129.07, 128.77, 123.20, 123.05, 119.45 (d, *J* = 3.2 Hz), 118.84, 116.48 (d, *J* = 22.1 Hz), 109.11, 38.48, 38.08.

2-((2-(Benzylthio)-1*H*-benzimidazol-1-yl)methyl)-5-(4-methoxyphenyl)-1,3,4-oxadiazole (**Compound 3**)

Prepared according to the general procedure from intermediate **A3** (312 mg, 1.0 mmol) and 4-methoxybenzoic acid (228 mg, 1.5 mmol). Yield: 93 mg (22%); white solid. Mp 156.0-156.5 °C.

HRMS (ESI) *m*/*z*: calcd for $C_{24}H_{21}N_4O_2S$ $[M+H]^+$ 429.1385; found 429.1394. IR (ATR, cm^{-1}): 3067, 3033, 2978, 2930, 2830, 1607, 1492, 1442, 1273, 1237, 1170, 1030, 842, 817, 759, 732, 695. ^1H NMR (500 MHz, $CDCl_3$) δ 7.84 (d, *J* = 9.0 Hz, 2H), 7.75 (d, *J* = 6.6 Hz, 1H), 7.44 (d, *J* = 8.5 Hz, 1H), 7.40 (d, *J* = 7.2 Hz, 2H), 7.32-7.21 (m, 5H), 6.94 (d, *J* = 9.0 Hz, 2H), 5.46 (s, 2H), 4.66 (s, 2H), 3.85 (s, 3H). ^{13}C NMR (126 MHz, $CDCl_3$) δ 165.83, 162.64, 160.11, 151.05, 136.52, 135.49, 129.08, 128.88, 128.76, 127.87, 123.14, 122.96, 118.80, 115.58, 114.51, 109.21, 55.47, 38.55, 38.12.

2-((2-(Benzylthio)-1*H*-benzimidazol-1-yl)methyl)-5-(4-nitrophenyl)-1,3,4-oxadiazole (**Compound 4**)

Prepared according to the general procedure from intermediate **A3** (624 mg, 2.0 mmol) and 4-nitrobenzoic acid (501 mg, 3.0 mmol). Yield: 107 mg (12%); pale yellow solid. Mp 157.2-158.0 °C. HRMS (ESI) *m*/*z*: calcd for $C_{23}H_{18}N_5O_3S$ $[M+H]^+$ 444.1130; found 444.1134. IR (ATR, cm^{-1}): 3109, 3060, 2977, 2927, 1608, 1554, 1521, 1445, 1349, 1334, 1295, 1231, 1161, 1083, 1011, 854, 770, 742, 703. ^1H NMR (500 MHz, $CDCl_3$) δ 8.31 (d, *J* = 9.0 Hz, 2H), 8.08 (d, *J* = 8.9 Hz, 2H), 7.76 (d, *J* = 8.5 Hz, 1H), 7.47–7.37 (m, 3H), 7.35–7.23 (m, 5H), 5.52 (s, 2H), 4.67 (s, 2H). ^{13}C NMR (126 MHz, $CDCl_3$) δ 164.12, 161.67, 150.99, 149.82, 136.52, 135.37, 129.07, 128.80, 128.53, 128.06, 127.95, 124.38, 123.29, 123.17, 118.94, 108.96, 38.42, 38.07.

Cell viability assay using MTT method

MCF-7 (human breast adenocarcinoma), MDA-MB-468 (human triple-negative breast adenocarcinoma), and A549 (human lung adenocarcinoma) cells were seeded into 96-well plates and cultured to approximately 70% confluence. Cells were then treated with compounds **1**-**4** at concentrations of 1, 3, 10, 30, and 100 μM. All compounds were dissolved in DMSO, with the final DMSO concentration maintained at 0.2%. After 48 h of exposure, cellular morphology was examined by phase-contrast microscopy, followed by assessment of cell viability using the MTT assay (Simay Demir, Mohammed Ahmed, Tayyar, Ozdemir, & Ark, 2025). Cell viability was expressed relative to the untreated control. Statistical analysis was performed using one-way ANOVA followed by Tukey's post hoc test ($p < 0.05$).

DPPH radical scavenging activity assay

The DPPH radical scavenging activity of the compounds was evaluated according to the method reported by Blois (1958), with slight modifications. Briefly, the test compounds were screened at final concentrations of 30, 100, and 300 μM, while gallic acid was used as the reference antioxidant. For the assay, 20 μL of each sample solution was mixed with 180 μL of DPPH solution in ethanol (0.15 mM). The mixtures were incubated at room temperature for 30 min in the dark, and the absorbance was then measured at 517 nm. The radical scavenging activity was calculated using the equation: [(A_control − A_sample)/A_control] × 100, where A_control represents the absorbance of the DPPH solution without sample, and A_sample corresponds to the absorbance measured in the presence of the test compound or gallic acid. All experiments were carried out in triplicate, and the results were expressed as mean ± SD.

RESULTS AND DISCUSSION

Chemistry

The synthetic route adopted for the preparation of the title benzimidazole–oxadiazole hybrids (**1**-**4**) is il-

lustrated in Figure 2. The molecular design was based on the integration of two biologically relevant heterocyclic pharmacophores, benzimidazole and 1,3,4-oxadiazole, into a single framework through a methylene linker. Such a hybridization approach has frequently been employed in medicinal chemistry to combine favorable structural features of individual pharmacophores within a unified scaffold. In the present study, a series of 2-((2-(benzylthio)-1*H*-benzimidazol-1-yl) methyl)-5-aryl-1,3,4-oxadiazole derivatives bearing aryl substituents with distinct electronic properties were synthesized and fully characterized.

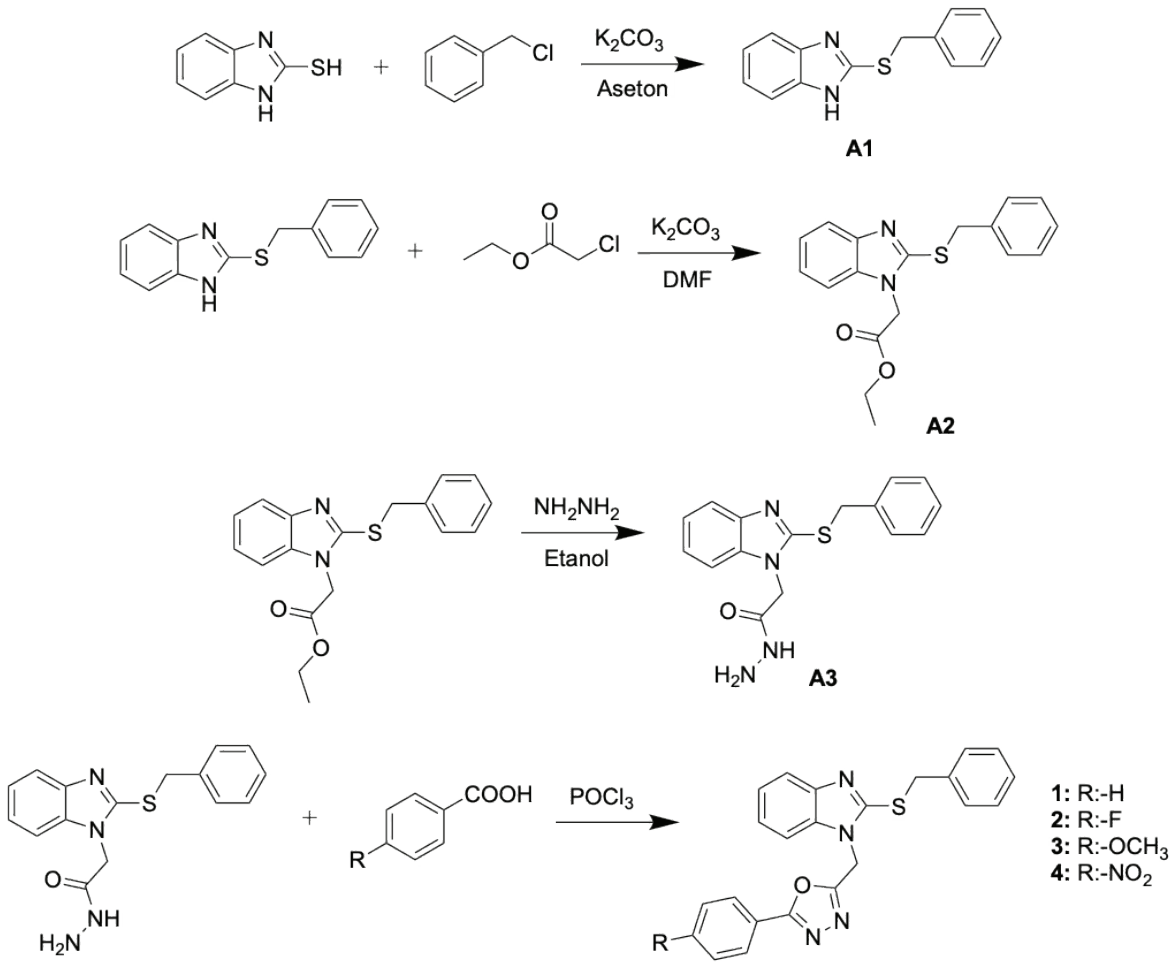

Figure 2. Synthesis route of title compounds (**1**-**4**)

The synthesis commenced with selective S-benzylation of 2-mercaptobenzimidazole to afford intermediate **A1**. Subsequent *N*-alkylation with ethyl chloroacetate introduced the methylene spacer required for the final molecular architecture and yielded ester intermediate **A2**. Conversion of the ester functionality into the corresponding hydrazide **A3** was accomplished using hydrazine hydrate. This intermediate served as the key precursor for the construction of the 1,3,4-oxadiazole ring system. Cyclodehydration of **A3** with the appropriate substituted benzoic acids in the presence of phosphorus oxychloride successfully afforded the desired target compounds **1**-**4**. In this transformation, $POCl_3$ acted both as a dehydrating and cyclization reagent, promoting efficient ring closure and formation of the oxadiazole nucleus. The em-

ployed synthetic strategy tolerated both electron-donating and electron-withdrawing substituents on the aromatic ring, enabling the preparation of structurally diverse analogues. Thus, unsubstituted phenyl (**1**), 4-fluorophenyl (**2**), 4-methoxyphenyl (**3**), and 4-nitrophenyl (**4**) derivatives were obtained. Although the final cyclization step furnished the title compounds in modest isolated yields (12-22%), the desired products were obtained in analytically pure form after chromatographic purification. The relatively low isolated yields may be associated with the harsh dehydrative conditions employed during oxadiazole ring formation together with material losses occurring during the two-step chromatographic purification process.

The structures of all synthesized compounds were unambiguously established by FT-IR, ^{1}H NMR, ^{13}C NMR, and HRMS analyses. The FT-IR spectra provided initial evidence for successful cyclization. In particular, the disappearance of the characteristic hydrazide carbonyl absorption expected for intermediate **A3** and the presence of strong absorptions around 1600-1610 cm^{-1} were consistent with formation of the 1,3,4-oxadiazole framework. Furthermore, substituent-specific absorptions were observed for individual derivatives. Compound **4** displayed characteristic nitro group stretching vibrations at 1521 and 1334 cm^{-1}, while compound **3** exhibited bands attributable to the methoxy substituent at 1273 and 1030 cm^{-1}. The ^{1}H NMR spectra of compounds **1**-**4** further confirmed the proposed structures. A characteristic singlet corresponding to the benzylic methylene protons attached to sulfur was consistently observed at δ 4.66-4.69 ppm, whereas the methylene linker connecting the benzimidazole and oxadiazole moieties appeared as a singlet at δ 5.46-5.52 ppm. The persistence of these two resonances throughout the series clearly demonstrated that both structural fragments remained intact during the cyclization process. In addition, aromatic proton signals arising from the benzimidazole, benzyl, and aryl substituents appeared within the expected chemical shift ranges. The electronic nature of the para-substituent exerted a noticeable influence on the aromatic proton resonances. The methoxy-substituted derivative **3** displayed relatively upfield aromatic signals owing to the electron-donating character of the methoxy group. In contrast, the nitro-substituted derivative **4** exhibited the most downfield aromatic resonances, with the para-substituted phenyl protons appearing at δ 8.31 and 8.08 ppm. This pronounced deshielding effect is consistent with the strong electron-withdrawing nature of the nitro substituent and provides additional support for the assigned structures. The ^{13}C NMR spectra were fully consistent with the formation of the target oxadiazole derivatives. Characteristic resonances corresponding to the C=N-containing carbons of the 1,3,4-oxadiazole ring were observed in the δ 160–166 ppm region for all compounds. Signals attributable to aromatic carbons and methylene carbons were also detected at the expected chemical shifts. Particularly noteworthy was compound **2**, in which the carbon directly bonded to fluorine appeared as a doublet with a large carbon–fluorine coupling constant (J_{CF} = 253.9 Hz). Such a coupling pattern is characteristic of aromatic fluorinated systems and provided strong spectroscopic evidence for successful incorporation of the fluorine substituent. High-resolution mass spectrometric analysis further confirmed the identities of the synthesized compounds. In all cases, the experimentally observed protonated molecular ion peaks $[M+H]^{+}$ showed excellent agreement with the calculated exact masses. The observed mass deviations were within the acceptable range for high-resolution measurements, thereby providing strong confirmation of the proposed molecular formulas.

In vitro biological activity

The biological activity of compounds **1**-**4** was evaluated using the MTT assay against A549 lung adenocarcinoma, MCF-7 estrogen receptor-positive breast cancer, and MDA-MB-468 triple-negative breast cancer cell lines. Doxorubicin was used as the reference anticancer drug, while untreated and DMSO-treated cells served as control groups. In addition to cell viability measurements, phase-contrast microscopic images were examined to support the quantitative findings.

The synthesized compounds showed a clear cell line-dependent response. In A549 cells, compounds **1**-**4** did not cause a meaningful reduction in cell viability at 100 µM (Figure 3.). While doxorubicin at 10 µM reduced cell viability to 18.75%, the viability of A549 cells treated with the synthesized compounds remained close to the control group, approximately within the range of 95-100%. Microscopic examination was consistent with these results, as A549 cells treated with the compounds largely preserved their typical adherent morphology and cell density. In contrast, doxorubicin-treated cells showed evident cytotoxic changes, including cell rounding, shrinkage, and loss of adherence. These findings indicate that the synthesized benzimidazole-1,3,4-oxadiazole hybrids were essentially inactive against A549 cells under the tested conditions.

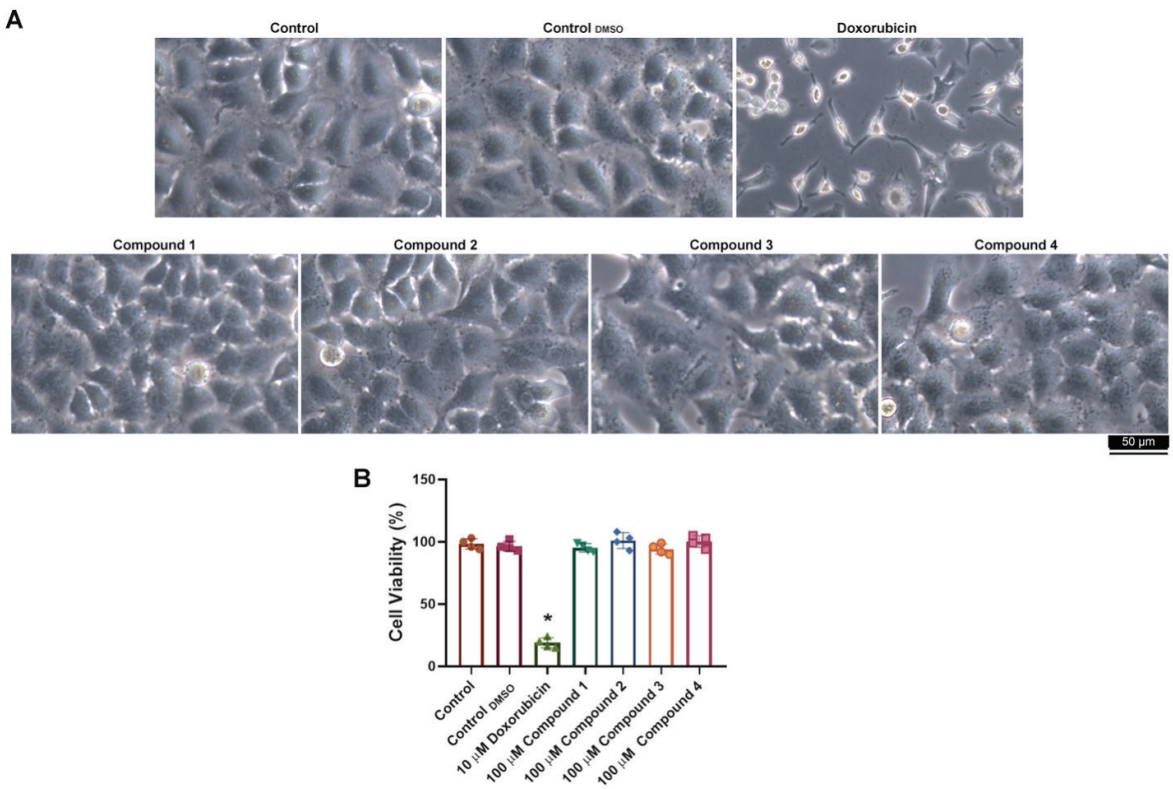

Figure 3. Antiproliferative effects of benzimidazole-1,3,4-oxadiazole hybrids on A549 lung cancer cells. (**A**) Representative phase-contrast images of A549 cells treated with control, DMSO, doxorubicin, and compounds **1**-**4**, showing treatment-related morphological changes. Scale bar: 50 µm. (**B**) Comparative cell viability of A549 cells treated with 10 µM doxorubicin or 100 µM compounds **1**-**4**. Data are expressed as mean ± SD

A different response was observed in breast cancer cells. In MCF-7 cells, compounds **1**-**4** reduced cell viability to 44.25%, 57.25%, 37.75%, and 61.25%, respectively, at 100 µM (Figure 4.). Although the synthesized compounds were less potent than the reference drug, they produced a clear and reproducible reduction in MCF-7 cell viability. Among the series, compound **3**, bearing a para-methoxy substituent, showed the most pronounced effect, followed by compound **1**. These findings were supported by phase-contrast microscopy, which demonstrated marked morphological changes in treated cells, including cell rounding, decreased spreading, partial loss of adhesion to the culture surface, cell detachment, and occasional membrane blebbing, compared with the control group.

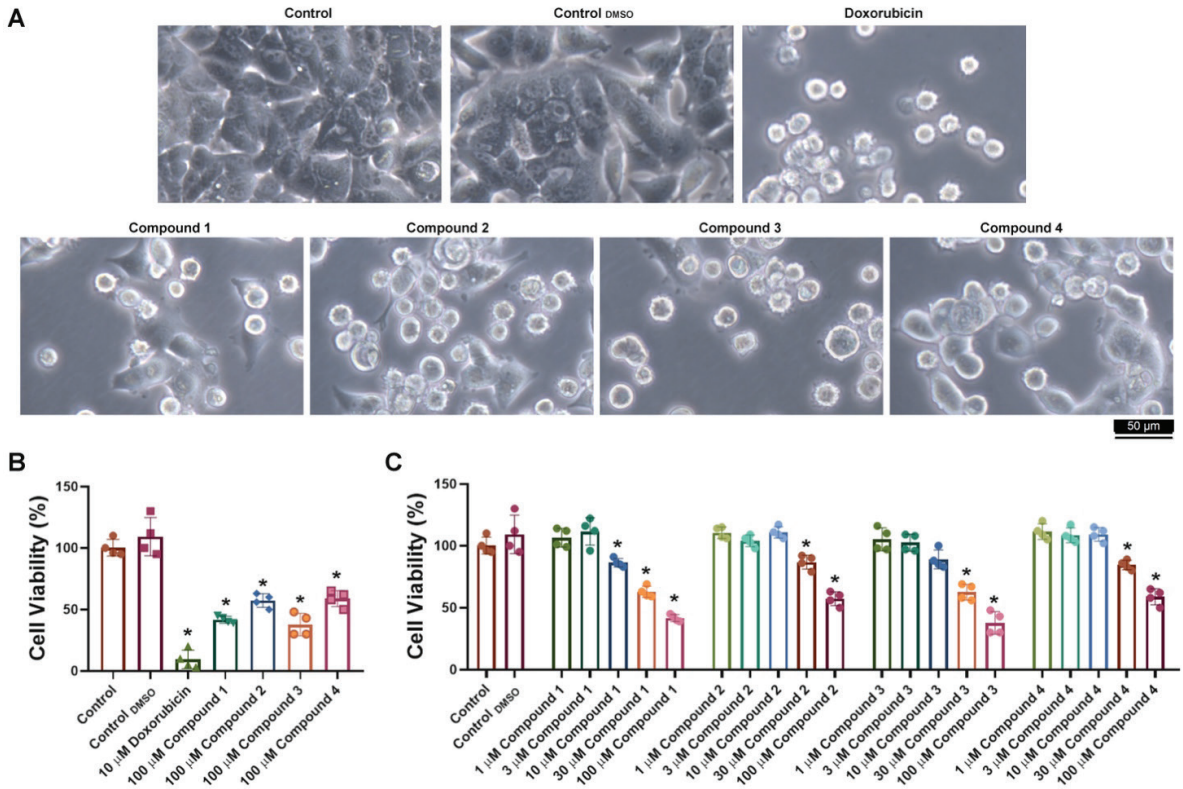

Figure 4. Antiproliferative effects of benzimidazole-1,3,4-oxadiazole hybrids on MCF-7 breast cancer cells. (**A**) Representative phase-contrast images of MCF-7 cells treated with control, DMSO, doxorubicin, and compounds **1**-**4**, showing treatment-related morphological changes. Scale bar: 50 µm. (**B**) Comparative cell viability of MCF-7 cells treated with 10 µM doxorubicin or 100 µM compounds **1**-**4**. (**C**) Dose-dependent effects of compounds **1**-**4** on MCF-7 cell viability. Data are expressed as mean ± SD. *$p < 0.05$ vs. control

The compounds also displayed moderate antiproliferative activity against MDA-MB-468 cells. At 100 µM, cell viability values were 46.25%, 61.00%, 39.00%, and 45.00% for compounds **1**-**4**, respectively (Figure 5.). Similar to the MCF-7 results, compound **3** was the most active derivative in this cell line. Compounds **1** and **4** showed comparable intermediate activity, whereas compound **2**, containing a para-fluoro substituent, was the least active compound in both breast cancer cell lines. The microscopic images supported the MTT results, showing reduced cell density and treatment-related morphological changes in breast cancer cells, particularly after treatment with the more active derivatives.

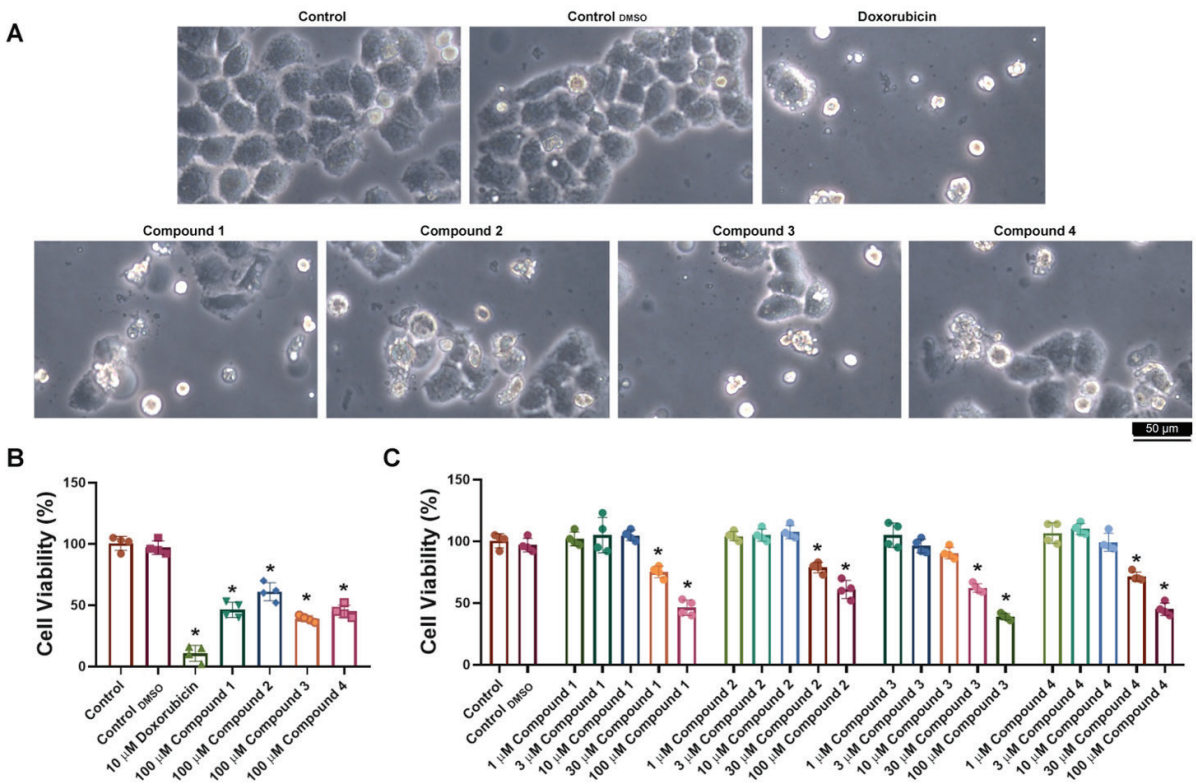

Figure 5. Antiproliferative effects of benzimidazole-1,3,4-oxadiazole hybrids on MDA-MB-468 triple-negative breast cancer cells. (**A**) Representative phase-contrast images of MDA-MB-468cells treated with control, DMSO, doxorubicin, and compounds **1**-**4**, showing treatment-related morphological changes. Scale bar: 50 µm. (**B**) Comparative cell viability of MDA-MB-468 cells treated with 10 µM doxorubicin or 100 µM compounds **1**-**4**. (**C**) Dose-dependent effects of compounds **1**-**4** on MDA-MB-468 cell viability. Data are expressed as mean ± SD. *$p < 0.05$ compared with the untreated control

The overall biological profile suggests that these compounds do not behave as broadly cytotoxic molecules. Instead, they appear to show a preferential antiproliferative response toward breast cancer cell lines compared with A549 lung cancer cells. This observation is noteworthy because MCF-7 and MDA-MB-468 cells represent biologically distinct breast cancer models. MCF-7 cells are estrogen receptor-positive and luminal-like, whereas MDA-MB-468 cells are commonly used as a triple-negative/basal-like breast cancer model. Therefore, the activity observed in both cell lines may indicate that the synthesized scaffold affects cellular mechanisms that are relevant to breast cancer cell survival but are not strictly dependent on estrogen receptor status.

A preliminary structure-activity relationship can also be proposed from the obtained data. The para-methoxy-substituted compound **3** consistently exhibited the most favorable activity profile in both breast cancer cell lines, reducing cell viability to 37.75% in MCF-7 and 39.00% in MDA-MB-468 cells. This suggests that an electron-donating substituent on the aryl ring of the oxadiazole moiety may contribute positively to the antiproliferative activity of this scaffold. In contrast, the para-fluoro derivative **2** showed the weakest activity, indicating that fluorine substitution at this position was not advantageous in the present series. The unsubstituted compound **1** and the para-nitro derivative **4** displayed intermediate effects, suggesting that both neutral and electron-withdraw-

ing aryl substitution patterns are tolerated but do not improve activity to the same extent as the methoxy group.

The radical scavenging potential of compounds **1**-**4** was also assessed using the DPPH assay. However, none of the synthesized compounds showed notable DPPH radical scavenging activity under the tested conditions. This negative result is still informative, as it suggests that the antiproliferative effects observed in MCF-7 and MDA-MB-468 cells are unlikely to be directly associated with classical free radical scavenging or antioxidant behavior. Therefore, the cytotoxic response of these benzimidazole-1,3,4-oxadiazole hybrids may be related to alternative cellular mechanisms rather than direct antioxidant activity.

Taken together, the biological findings identify compound **3** as the most promising analogue of the series and suggest that the benzimidazole-1,3,4-oxadiazole hybrid scaffold may serve as a useful starting point for the development of breast cancer-oriented antiproliferative candidates.

CONCLUSION

In conclusion, four benzylthio-substituted benzimidazole-1,3,4-oxadiazole hybrids were successfully synthesized and structurally characterized. The title compounds were obtained through a rational multistep synthetic route that enabled the combination of benzimidazole and 1,3,4-oxadiazole pharmacophores within the same molecular framework. The spectroscopic and spectrometric data supported the proposed structures and confirmed the successful formation of the designed hybrid scaffold. The biological evaluation revealed a clear cell line-dependent activity profile. Compounds **1**-**4** were essentially inactive against A549 lung adenocarcinoma cells at 100 μM, whereas they showed moderate antiproliferative effects against both MCF-7 and MDA-MB-468 breast cancer cells. This difference suggests that the compounds may not act as nonspecific cytotoxic agents, but rather may produce a preferential response in breast cancer cell models. Among the synthesized derivatives, compound **3**, containing a para-methoxy substituent on the aryl ring of the oxadiazole moiety, was the most active analogue in both breast cancer cell lines. This finding indicates that electron-donating substitution may have a favorable influence on the biological activity of this scaffold. The lack of notable DPPH radical scavenging activity suggests that the observed antiproliferative effects are unlikely to be explained by direct antioxidant behavior. Therefore, other cellular mechanisms may be involved in the response of breast cancer cells to these compounds. Although the activity of the synthesized derivatives was moderate compared with doxorubicin, their distinct response profile across different cancer cell lines makes this chemical series worthy of further investigation. Overall, the present study provides a useful foundation for the further optimization of benzimidazole-1,3,4-oxadiazole hybrids as breast cancer-oriented antiproliferative candidates.

ACKNOWLEDGEMENTS

Financial support by the Scientific and Technological Research Council of Turkey (TUBITAK 2209-A program) under Grant 1919B012420588 is gratefully acknowledged.

AUTHOR CONTRIBUTION STATEMENT

Design, supervision, and DPPH assay (MG), synthesis and structure elucidation of the compounds (MG and ŞY), MTT assay (YDŞD and ZA). All authors reviewed and edited the manuscript. All authors read and approved the manuscript.

CONFLICT OF INTEREST

The authors declare that there is no conflict of interest.

REFERENCES

Abd El-Meguid, E. A., Awad, H. M., & Anwar, M. M. (2019). Synthesis of New 1,3,4-Oxadiazole-benzimidazole Derivatives as Potential Antioxidants and Breast Cancer Inhibitors with Apoptosis Inducing Activity. *Russian Journal of General Chemistry*, *89*(2), 348-356. https://doi.org/10.1134/S1070363219020282

Badawy, M. A. S., Bräse, S., Ali, T. F. S., Abdel-Aziz, M., & Abdel-Rahman, H. M. (2025). Biologically Active Benzimidazole Hybrids as Cancer Therapeutics: Recent Advances. *Pharmaceuticals*, *18*(10), 1454.

Blois, M. S. (1958). Antioxidant Determinations by the Use of a Stable Free Radical. *Nature*, *181*(4617), 1199-1200. https://doi.org/10.1038/1811199a0

Bray, F., Laversanne, M., Sung, H., Ferlay, J., Siegel, R. L., Soerjomataram, I., & Jemal, A. (2024). Global cancer statistics 2022: GLOBOCAN estimates of incidence and mortality worldwide for 36 cancers in 185 countries. *CA: A Cancer Journal for Clinicians*, *74*(3), 229-263. https://doi.org/https://doi.org/10.3322/caac.21834

Çevik, U. A., Celik, I., Görgülü, Ş., Şahin İnan, Z. D., Bostancı, H. E., Karayel, A.,…Kaplancıklı, Z. A. (2025). Novel Benzimidazole–Oxadiazole Derivatives as Anticancer Agents with VEGFR2 Inhibitory Activity: Design, Synthesis, In Vitro Anticancer Evaluation, and In Silico Studies. *ACS Omega*, *10*(7), 6801-6813. https://doi.org/10.1021/acsomega.4c08885

Dai, X., Cheng, H., Bai, Z., & Li, J. (2017). Breast Cancer Cell Line Classification and Its Relevance with Breast Tumor Subtyping [Review]. *Journal of Cancer*, *8*(16), 3131-3141. https://doi.org/10.7150/jca.18457

De Oliveira, C. S., Lira, B. F., Barbosa-Filho, J. M., Lorenzo, J. G. F., & De Athayde-Filho, P. F. (2012). Synthetic Approaches and Pharmacological Activity of 1,3,4-Oxadiazoles: A Review of the Literature from 2000–2012. *Molecules*, *17*(9), 10192-10231.

Foster, K. A., Oster, C. G., Mayer, M. M., Avery, M. L., & Audus, K. L. (1998). Characterization of the A549 Cell Line as a Type II Pulmonary Epithelial Cell Model for Drug Metabolism. *Experimental Cell Research*, *243*(2), 359-366. https://doi.org/https://doi.org/10.1006/excr.1998.4172

Glomb, T., Szymankiewicz, K., & Świątek, P. (2018). Anti-Cancer Activity of Derivatives of 1,3,4-Oxadiazole. *Molecules*, *23*(12), 3361.

Gunjan, B., Salahuddin, Avijit, M., Rajnish, K., Greesh, K., Mohamed Jawed, A.,…Bhupinder, K. (2024). Hybrids of Benzimidazole-oxadiazole: A New Avenue for Synthesis, Pharmacological Activity and Recent Patents for the Development of More Effective Ligands. *Current Organic Synthesis*, *21*(8), 976-1013. https://doi.org/http://dx.doi.org/10.2174/0115701794260740231010111408

Gupta, P., Verma, S., Narang, R., Sharma, B., Singh, V., & Lal, S. (2026). 1,3,4-Oxadiazole derivatives: targeting multiple bacterial pathways. *RSC Medicinal Chemistry*, *17*(4), 1867-1887. https://doi.org/10.1039/d5md01139f

Hagar, F. F., Abbas, S. H., Gomaa, H. A. M., Youssif, B. G. M., Sayed, A. M., Abdelhamid, D., & Abdel-Aziz, M. (2023). Chalcone/1,3,4-Oxadiazole/Benzimidazole hybrids as novel anti-proliferative agents inducing apoptosis and inhibiting EGFR & BRAFV600E. *BMC Chemistry*, *17*(1), 116. https://doi.org/10.1186/s13065-023-01003-3

Hagar, F. F., Abbas, S. H., Atef, E., Abdelhamid, D., & Abdel-Aziz, M. (2025). Benzimidazole scaffold as a potent anticancer agent with different mechanisms of action (2016–2023). *Molecular Diversity*, *29*(2), 1821-1849. https://doi.org/10.1007/s11030-024-10907-8

Kim, J., Harper, A., McCormack, V., Sung, H., Houssami, N., Morgan, E.,…Fidler-Benaoudia, M. M. (2025). Global patterns and trends in breast cancer incidence and mortality across 185 countries. *Nature Medicine*, *31*(4), 1154-1162. https://doi.org/10.1038/s41591-025-03502-3

Kumar, D., Patel, G., Chavers, A. K., Chang, K.-H., & Shah, K. (2011). Synthesis of novel 1,2,4-oxadiazoles and analogues as potential anticancer agents. *European Journal of Medicinal Chemistry*, *46*(7), 3085-3092. https://doi.org/https://doi.org/10.1016/j.ejmech.2011.03.031

Lalic, H., Aurer, I., Batinic, D., Visnjic, D., Smoljo, T., & Babic, A. (2022). Bendamustine: A review of pharmacology, clinical use and immunological effects (Review). *Oncol Rep*, *47*(6). https://doi.org/10.3892/or.2022.8325

Lee, Y. T., Tan, Y. J., & Oon, C. E. (2023). Benzimidazole and its derivatives as cancer therapeutics: The potential role from traditional to precision medicine. *Acta Pharmaceutica Sinica B*, *13*(2), 478-497. https://doi.org/https://doi.org/10.1016/j.apsb.2022.09.010

Nachman, S., Zheng, N., Acosta, E. P., Teppler, H., Homony, B., Graham, B.,…Laurel, B. (2014). Pharmacokinetics, Safety, and 48-Week Efficacy of Oral Raltegravir in HIV-1–Infected Children Aged 2 Through 18 Years. *Clinical Infectious Diseases*, *58*(3), 413-422. https://doi.org/10.1093/cid/cit696

Perou, C. M., Sørlie, T., Eisen, M. B., van de Rijn, M., Jeffrey, S. S., Rees, C. A.,…Botstein, D. (2000). Molecular portraits of human breast tumours. *Nature*, *406*(6797), 747-752. https://doi.org/10.1038/35021093

Quy, N. P., Hue, B. T. B., Do, K. M., Quy, H. T. K., De, T. Q., Phuong, T. T. B.,…Morita, H. (2022). Design, Synthesis and Cytotoxicity Evalufation of Substituted Benzimidazole Conjugated 1,3,4-Oxadiazoles. *Chemical and Pharmaceutical Bulletin*, *70*(6), 448-453. https://doi.org/10.1248/cpb.c22-00162

Shajari, N., & Eskandari, P. (2026). A comprehensive overview of the recent development of privileged 1, 3, 4-oxadiazole derivatives and their biological activities. *Journal of Molecular Structure*, *1349*, 143639. https://doi.org/https://doi.org/10.1016/j.molstruc.2025.143639

Simay Demir, Y. D., Mohammed Ahmed, I., Tayyar, T., Ozdemir, A., & Ark, M. (2025). Targeting SASP with FDA-approved agents: minoxidil and diazoxide as potential senomorphic agents in cancer therapy. *Turkish Journal of Biochemistry*, *50*(6), 947-958. https://doi.org/doi:10.1515/tjb-2025-0249

Singh, A. K., Kumar, A., Singh, H., Sonawane, P., Paliwal, H., Thareja, S.,…Kumar, P. (2022). Concept of Hybrid Drugs and Recent Advancements in Anticancer Hybrids. *Pharmaceuticals*, *15*(9), 1071.

Stecoza, C. E., Nitulescu, G. M., Draghici, C., Caproiu, M. T., Olaru, O. T., Bostan, M., & Mihaila, M. (2021). Synthesis and Anticancer Evaluation of New 1,3,4-Oxadiazole Derivatives. *Pharmaceuticals*, *14*(5), 438.

Subik, K., Lee, J. F., Baxter, L., Strzepek, T., Costello, D., Crowley, P.,…Tang, P. (2010). The Expression Patterns of ER, PR, HER2, CK5/6, EGFR, Ki-67 and AR by Immunohistochemical Analysis in Breast Cancer Cell Lines. *Breast Cancer (Auckl)*, *4*, 35-41.

Tsukumo, Y., Naito, M., & Suzuki, T. (2020). Influence of EGFR-activating mutations on sensitivity to tyrosine kinase inhibitors in a KRAS mutant non-small cell lung cancer cell line. *PLoS One*, *15*(3), e0229712. https://doi.org/10.1371/journal.pone.0229712

Werner Alyssa, N., Kumar Avani, I., Charest Pascale, G., & Welch, M. (2023). CRISPR-mediated reversion of oncogenic KRAS mutation results in increased proliferation and reveals independent roles of Ras and mTORC2 in the migration of A549 lung cancer cells. *Molecular Biology of the Cell*, *34*(13), ar128. https://doi.org/10.1091/mbc.E23-05-0152

Yin, L., Duan, J.-J., Bian, X.-W., & Yu, S.-C. (2020). Triple-negative breast cancer molecular subtyping and treatment progress. *Breast Cancer Research*, *22*(1), 61. https://doi.org/10.1186/s13058-020-01296-5

Zagami, P., & Carey, L. A. (2022). Triple negative breast cancer: Pitfalls and progress. *npj Breast Cancer*, *8*(1), 95. https://doi.org/10.1038/s41523-022-00468-0

Zhang, Y., Ji, Y., Liu, S., Li, J., Wu, J., Jin, Q.,…Huang, Y. (2025). Global burden of female breast cancer: new estimates in 2022, temporal trend and future projections up to 2050 based on the latest release from GLOBOCAN. *Journal of the National Cancer Center*, *5*(3), 287-296. https://doi.org/https://doi.org/10.1016/j.jncc.2025.02.002